Analysis of filament wound pressure tanks considering fiber angle variation in thickness direction

Jae-sung Park [1], Cheol-ung Kim [1], Chang-Sun Hong [1], Chun-Gon Kim[1] and Tae-Kyung Hwang[2]

[1] *Department of Aerospace Engineering, Korea Advanced Institute of Science & Technology*
373-1, Kusong-dong, Yusong-gu, Taejon 305-701, KOREA:cronus@kaist.ac.kr
[2] *Agency for Defense Development*
Yusong P.O.Box 35, Taejon, 305-600, KOREA

SUMMARY: In this study filament winding patterns are simulated using semi-geodesic fiber path equation for an arbitrary surface. As the fiber path depends on the surface where fibers are wound, the fiber angle varies in the longitudinal and thickness directions of a pressure tank. Finite element analyses are performed considering fiber angle variation in the longitudinal and thickness directions by ABAQUS. From the stress results of pressure tanks, maximum stress criterion in the transverse direction is applied to modify material properties of failed region. At the end of each load increment, resultant layer stresses are compared with a failure criterion and the mechanical properties are reduced to 1/10 for the failed layer. Results of progressive failure analysis are compared with two experimental data. Parametric studies such as the boss to cylinder radius ratio, R_b/R_c, thickness, and winding angle are done to investigate their effects on the performance of pressure tanks.

KEYWORDS: filament wound pressure tank, material nonlinearity, finite element analysis, ABAQUS

INTRODUCTION

As a part of several efforts to reduce overall weight of rockets and missiles, filament wound pressure tanks are replacing a portion of metallic materials traditionally used in manufacturing these tanks. The filament wound pressure tanks have remarkable properties in the specific modulus, thermal resistance and endurance compared with metallic fuel tanks. In spite of their good performance, pressure tanks made by filament winding have complex in analyzing the geometry and properties in their dome parts along a longitudinal axis. As fibers are wound on a cylindrical mandrel, curvilinear fiber path leads to continuous change in winding angle and thickness. Especially in the dome region, winding angles vary about 10 to 90 degrees and thickness about 1.4 to 20(mm) for a standard test and evaluation bottle (STEB). In addition, the fiber path depends on the surface which fibers are wound on, so that fiber angle varies in the thickness direction. Therefore finite element analyses including angle and thickness variation are required to predict the behavior of pressure tanks.

Isotensoid dome design[1], modified helically wound dome design[2] and planar wound dome design method[3] have been used generally to determine winding patterns and dome geometry.

Because previous methods calculate dome shape, winding angle, thickness simultaneously, initially determined winding patterns are maintained till the end of winding process. As the dome shape, winding angle and thickness distribution are determined from given the ratio of radius of cylinder to boss radius, and the fiber path on an arbitrary axisymmetric surface cannot be generated. In general, winding patterns change with increasing layers in dome part. The fiber path depends not only on the surface where the fibers are wound but also on the wound thickness. So fiber angle at the same axial position varies in the thickness direction during winding process. Hence the fiber angle must be re-calculated from changed thickness in the dome part during the winding process.

In the most of finite element analyses of filament wound pressure tanks, shell and axisymmetric solid elements are used [1,2,4]. For axisymmetric solid element, 3-dimensional effective moduli are needed and layerwise stress and strain are not available unless each layer is modeled respectively. Therefore reduction of material properties in layer level is not possible in progressive failure analysis. When shell elements are used in the analysis, detailed modeling of boss part is not easy and stress concentration between cylinder and dome part is sometimes overestimated.

Winding Pattern Calculation

Mandrel shape and winding path are determined using semi-geodesic fiber path equation. Slippage tendency(λ) considering the frictional force between wet tow and a mandrel is introduced to find possible winding patterns of the given arbitrary surface. The detailed derivation of equations can be found in the reference [5]. Fiber angle along the longitudinal axis can be calculated from the following equation.

$$\frac{d\alpha}{dx} = \frac{\lambda(A^2 \sin^2\alpha - rr''\cos^2\alpha) - r'A^2 \sin\alpha}{rA^2 \cos\alpha} \tag{1}$$

where α is the angle between the tangent to the fiber path and meridian of the surface, $r' = \frac{dr}{dx}$, $A = \sqrt{1+r'^2}$ (see Fig. 1)

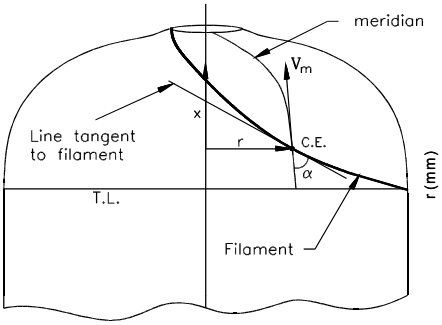

Fig. 1 Fiber angle variation

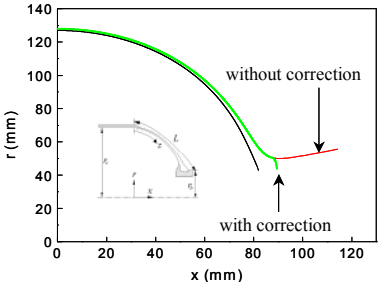

Fig. 2 Dome shape

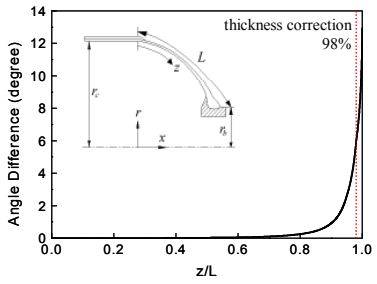

Fig. 3 Winding angle difference between first and last ply

The thickness of dome region can be computed from the generated winding patterns using Eqn (2).

$$t = \frac{r_c \cos\alpha_c}{r\cos\alpha} \times t_c \tag{2}$$

where r_c , α_c , t_c are radius, fiber angle, thickness of cylindrical region.

As the winding fiber approaches the boss of a mandrel, α becomes 90 degree. Right-hand side of Eqn (2) becomes infinity, and so does the thickness. Thickness divergence is caused by

fiber concentration on relatively small area. In other words, the fiber rotates repetitively near the boss before it winds to the opposite direction. Thus the wound thickness is corrected to be constant as $t \times r$ from 98 % of the meridian length measured from the cylinder-dome junction (see Fig. 2). To determine angle variation in the thickness direction, fiber path and thickness of the first ply are calculated beforehand from given mandrel shape. The second ply is wound on the top surface of the first ply. From summed thickness of previous plies, the fiber path and thickness of next ply can be generated up to the given number of plies. The angle difference between first and last ply is shown in Fig. 3

Finite Element Model with Material Nonlinearity

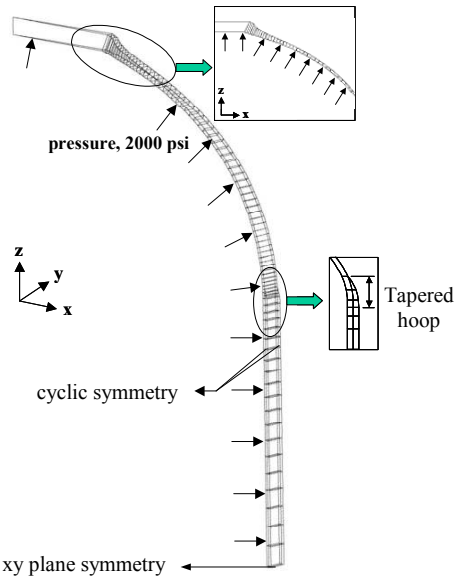

Fig. 4 Finite element model & B.C.

	Forward dome	Aft dome
Radius of cylinder, r_c	127.0 mm	
Radius of boss, r_b	45.80 mm	70.83 mm
Thickness of cylinder, t_c	1.4 mm	
Thickness of hoop, t_h	1.6 mm	

Table 1 Configuration of ASTEB

	Solid case	Failed case
E_1	161.3 Gpa	161.3 GPa
E_2, E_3	8.820 Gpa	0.882 GPa
G_{12}, G_{13}	5.331 Gpa	0.5331 GPa, 0.53GPa
G_{23}	2.744 Gpa	0.274 GPa
ν_{12}, ν_{13}	0.33	0.033, 0.33
ν_{23}	0.45	0.045
X_t	2300 Mpa	Used for burst prediction
X_c	1080 Mpa	
Y_t	30 Mpa	Used in failure criteria
Y_c	70 MPa	Used in failure criteria
density	1.5×10^{-6} kg/mm^3	

Table 2 Material properties of T800/Epoxy

In this study, three dimensional layered solid elements in ABAQUS are used to model an ASTEB (Advanced Standard Test Evaluation Bottle). The configuration of ASTEB and the material properties of T800/Epoxy are shown in Table 1-2. Finite element mesh is shown in Fig. 4. Total 85 layered solid elements are applied to model 3° strip of the tank by using cyclic symmetry condition. Internal pressure is increased to 2000 psi and degree of freedom in Z-direction is constrained to move along with the rigid boss at the end of dome element. As internal pressure is increasing, the rigid boss is gradually separating from the composite dome. Because detailed contact configuration between a metal boss and composite is not available, behavior near the boss may be inaccurate. As the failure of fiber means final burst in a filament winding pressure vessel, so that only transverse properties to the fiber are reduced to 10 % in the failed layers(see Table 2). After stresses calculated from the previous increment are compared with the strength of each layer, new modified material properties are used in next increment. In this case sudden property drop leads to difficulties in convergence and the accuracy of results often depends on the size of the time increment. Therefore small increments are used to stabilize solution path.

Performance Factor

Performance factor is introduced to evaluate the performance of each pressure tank [1].

$$performance\,factor = \frac{P \cdot V}{W}$$

where P, V, W are burst pressure, volume and weight of pressure tanks respectively. High burst pressure is desirable for given weight and capacity, so that reduction of winding thickness is required for higher performance factor. In order to decrease the thickness, maximum stress components must be found for the helical and hoop winding layers and layer thickness is controlled to reach the maximum stress in these layers simultaneously.

Result

Although it has been known that most of the stress is supported by fibers in filament wound pressure tanks, the properties reduction in the transverse direction raises fiber directional stress 5% higher. Fig. 5 shows that reduction of properties with higher pressure affects transverse stress distribution over a pressure tank. If stress components are higher than the maximum strength, moduli of these layers are reduced. Thus failed layers cannot support internal pressure any more, that is, stress components in these layers drop to nearly zero in the next increment.

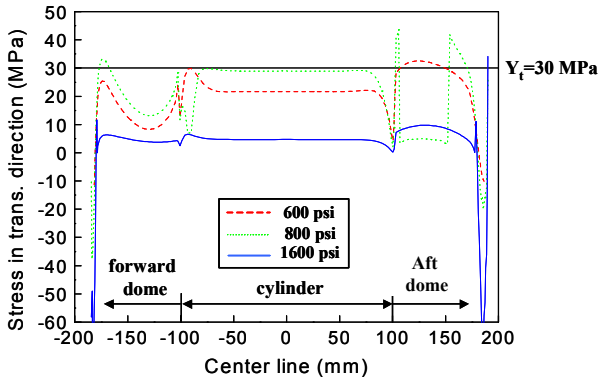

Fig. 5 Stress in transverse direction considering reduction of properties

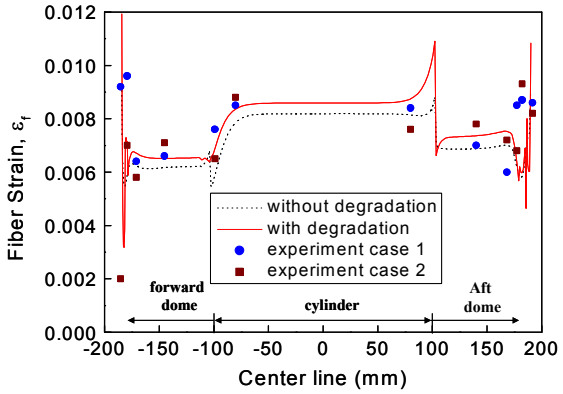

Fig. 6 Comparison of fiber strains between FEA & Experiment

Fig. 6 shows that FEA results are generally coincident with two experimental data. In addition, the model with degradation estimates fiber strain higher than that without degradation and progressive failure analysis leads to more accurate strain value. Strain fluctuates intensely in both ends of pressure tanks because severe boundary conditions are applied to simulate a metal boss as rigid constraints. Detailed contact modeling of the metal boss could improve the accuracy of FEA.

Design Modification of ASTEB

The Performance factor of given ASTEB (Table 1) varies 1.21×10^{6} - 1.54×10^{6} (in) according to its possible winding angles which are calculated from the radius ratio of cylinder to boss considering winding stability with slippage tendency (see in Fig. 6). Burst pressure is found among three layers (top surface of helical layer, bottom surface of hoop and helical layers). As you can see in Fig. 7, burst occurs in the junction of the backward dome and cylinder. Final

failure happens at the same position for all possible winding angles. That is, as winding angle is getting larger, burst pressure becomes higher. Therefore the pressure tank of the possible largest winding angle shows the best performance for a given geometry of ASTEB. If radius ratio of cylinder to boss changes, possible winding angles also become different. In this study, the given geometry of ASTEB leaves unchanged, winding angle and thickness of helical & hoop layers vary to find the highest performance factor. In that case, the most efficient design of pressure tanks is that of fiber directional stresses in all three layers reach the maximum at the same time (see Fig. 7).

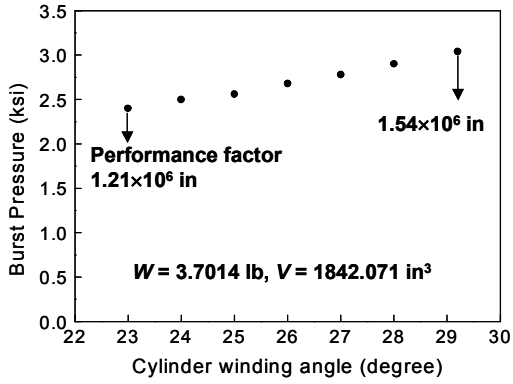

Fig. 6 Burst pressures of ASTEB with possible winding angles

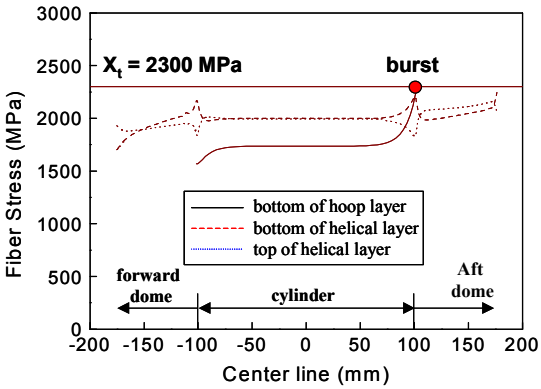

Fig. 7 Comparison of fiber stresses of ASTEB at p=3040 psi

	Winding angle of cylinder	t_c	t_h	Mass(lb)	Burst pressure	Performance factor	Remarks
ASTEB	27.5°	1.1 mm	1.2 mm	3.8706	2840 psi	1.35×10^6 in	Experiment case
ASTEB	29.2°	1.1 mm	1.2 mm	3.7014	3040 psi	1.54×10^6 in	Maximum case for ASTEB
Modified ASTEB	29.2°	0.9 mm	1.4 mm	3.5481	3500 psi	1.85×10^6 in	

Table 3 Comparison of performance factor

Performance factors of modified ASTEB are shown in Table 3. Performance of the tank used in the experiment can be improved as winding angle and thickness of hoop layer increase. However, thickness of helical layer is excessively thick and can be saved for better performance. In conclusion, the ASTEB with 29.2° winding angle, 0.9 mm helical layer and 1.4 mm hoop layer has about 37 % higher performance factor than the ASTEB used in the experiment.

CONCLUSIONS

In this study, performance factors of pressure tanks are evaluated with winding pattern and thickness of helical and hoop layers. Semi-geodesic fiber path equation is introduced to find a winding pattern on an arbitrary axisymmetric surface. In addition, fiber angle variation through the thickness direction is considered. Maximum stress criterion in the transverse direction is applied to assess matrix failure. Material properties are reduced in the failed element. Fiber directional stress becomes larger as failed elements increase in number. Accordingly entire stress level of pressure tanks grows higher.

In addition, the winding design is modified to improve efficiency of an ASTEB. Modified tanks show better performance comparing with the original ASTEB used in experiments. Winding angle increment and balancing in hoop and helical layer thickness not only enhance the performance but also result in higher burst pressure and lighter weight.

ACKNOWLEDGEMENT

This work was sponsored in part by KARI(Korea Aerospace Research Institute). The material properties and experimental data were provided by ADD(Agency for Defense Development). Their assistance is gratefully acknowledged.

REFERENCES

1. M. Uemura, "Developmental Research on Carbon-Fiber-Reinforced Plastic Rocket Motorcase," *The University of Tokyo, Report of Aerospace Research Center*, Vol. 15, No. 4, 1979

2 Y. D. Doh, and C. S. Hong, "Progressive Failure Analysis for Filament Wound Pressure Vessel," *Journal of Reinforced Plastics and Composites*, Vol. 14, No. 12, pp.1278-1306, 1995

3 R. F. Hartung, "Planar-wound Filamentary Pressure Vessels," *AIAA Journal*, Vol. 1, 1963, pp. 2842-2844

4 L. Lemoine, "Effects of Geometrical and Material Nonlinearities on Deflections of Filament-wound Motor Chambers," *AIAA* 78-1565, 1978

5 J. Scholliers and H. Van Brussel, "Computer-integrated filament winding: computer-integrated design, robotic filament winding and robotic quality control," *Composites Manufacturing*, Vol.5, No. 1, 1994, pp. 15-23